Available online at www.sciencedirect.com
SCIENCE DIRECT®
Journal of Organometallic Chemistry 690 (2005) 4132–4138
Journal of Organometallic Chemistry
www.elsevier.com/locate/jorganchem

TR-FTIR absorption spectroscopy of transition metal carbonyl radicals generated by photodissociation of metal–metal bonds, by halogen abstraction or by radical ligand substitution

Thiam Seong Chong, Peng Li, Weng Kee Leong, Wai Yip Fan *

Department of Chemistry, National University of Singapore, 3 Science Drive 3, Singapore 117543, Singapore

Received 30 April 2005; received in revised form 6 June 2005; accepted 16 June 2005

Abstract

Three methods of obtaining time-resolved Fourier-Transform infrared (TR-FTIR) absorption spectra of transition metal carbonyl radicals in hexane are reported here. For the first method, $CpM(CO)_2L$ and $Cp^*M(CO)_2L$ (M = Mo, W; L = CO, PR_3) radicals have been generated by photodissociation of the corresponding metal–metal bonded dimers. Radicals of formula $M(CO)_4L$ (M = Mn, Re; L = CO, PR_3, $AsPh_3$, $SbPh_3$) and $CpM(CO)_n$ (M = Fe, Mo; $n = 2$, 3) have been produced via the second method which is halogen abstraction of the transition metal carbonyl halides using $CpMo(CO)_3$ radical. For the third method, fast radical ligand substitution kinetics has been exploited to generate $CpMo(CO)_2PR_3$ radicals from $CpMo(CO)_3$ in the presence of free phosphines. An assessment of the three methods with respect to TR-FTIR spectroscopic detection of radicals was also discussed.

Keywords: TR-FTIR radical spectra; Metal–metal bond dissociation; Halide abstraction; Ligand substitution kinetics

1. Introduction

The direct observation of 17-electron transition metal carbonyl radicals and other reactive intermediates using time-resolved infrared spectroscopy (TRIR) has continued to receive much attention [1–6]. This technique has often been applied to the detection of $CpM(CO)_nL$ [M = Fe, Mo, W; $n = 2$, 3; L = CO, PR_3 (for Fe only)] and $M(CO)_5$ (M = Mn, Re) radicals produced via photolysis of metal–metal bonded dimers [7–13]. The advent of time-resolved Fourier-Transform infrared (TR-FTIR) absorption technique has further widened the scope for simultaneous detection of radical spectra across the mid-IR region [14]. TR-FTIR techniques could be invaluable for determining lifetimes and reaction rates of key radical intermediates directly implicated in transition metal carbonyl-catalysed reactions [15–17].

In this work, we focus on obtaining TR-FTIR spectroscopic data of transition metal carbonyl radicals by utilising three different methods of radical production. Firstly, photodissociation of metal-bonded dimers has continued to be a convenient way of acquiring spectra of radicals such as $CpM(CO)_2PR_3$ or $Cp^*M(CO)_3$ [M = Mo, W]. Secondly, radicals generated via halogen abstraction of transition metal carbonyl halides by $CpMo(CO)_3$ have turned out to be suitable candidates for TR-FTIR studies. This method is especially useful for studying $M(CO)_4(EPh_3)$ (M = Mn, Re; E = P, As, Sb) radicals without the concomitant presence of decarbonylation products. Thirdly, we have made use of fast radical ligand substitution kinetics to generate phosphine derivatives of $CpMo(CO)_3$ itself. For the second and third methods, $CpMo(CO)_3$ has to be generated

* Corresponding author. Tel.: +65 68746823/96385110; fax. +65 67791691.
E-mail address: chmfanwy@nus.edu.sg (W.Y. Fan).

0022-328X/$ - see front matter © 2005 Elsevier B.V. All rights reserved.
doi:10.1016/j.jorganchem.2005.06.015

in situ first by visible laser photolysis. The suitability of all three methods towards detection of certain classes of transition metal carbonyl radicals will be discussed. Although a wealth of kinetic data could be extracted from TR-FTIR studies, we have left the detail analysis of the reaction rates and lifetimes of radicals to a forthcoming paper. Only brief observations pertaining to radical kinetics will be mentioned here.

2. Experiment

A brief description of the cell used for performing time-resolved and linear FTIR spectroscopy on the reaction mixture is given here (see Fig. 1). It is a stainless steel, static, liquid cell with CaF_2 windows for passage of the IR probe beam. Absorbance pathlengths of 0.2–5 mm could be accommodated by manual adjustment of the window holders. The cell also allowed for placement of quartz or glass windows to permit photodissociation by a laser beam propagated at right angle to the IR probe beam. The cell could hold a volume of about 40 ml of solvent, together with a magnetic bar to provide constant stirring. Inlet and outlet ports on each side of the cell allowed for N_2 bubbling through the solution if required.

The sample preparations for all three methods were carried out in the dark under nitrogen atmosphere. The precursors $Cp_2Mo_2(CO)_5PR_3$, $[CpM(CO)_2PR_3]_2$, $[Cp^*M(CO)_2PR_3]_2$ (M = Mo or W; R = Ph, OEt, Me) and $M(CO)_4EPPh_3Br$ (M = Mn, Re; E = P, As, Sb) compounds were prepared according to literature methods [18–22]. All other organometallic compounds obtained from Strem and Aldrich were used directly without purification. For method 1, the metal–metal bonded precursor was dissolved in hexane and transferred into the air-tight IR cell with the optical pathlength set at 2 mm. Usually about 10–20 mg of the precursor in 30 ml solvent (10^{-2}–10^{-3} M) was sufficient to generate free radical spectra. For the second method, a quantity of $[CpMo(CO)_3]_2$ was added into the hexane solution already containing the transition metal carbonyl halides. Again the same concentrations of precursors of 10^{-2}–10^{-3} M have been used for this method. However since the reactions are irreversible, the precursor concentration could be depleted very quickly depending on the laser pulse energy. Hence if the concentrations of radicals had to be maintained for longer observations, saturated

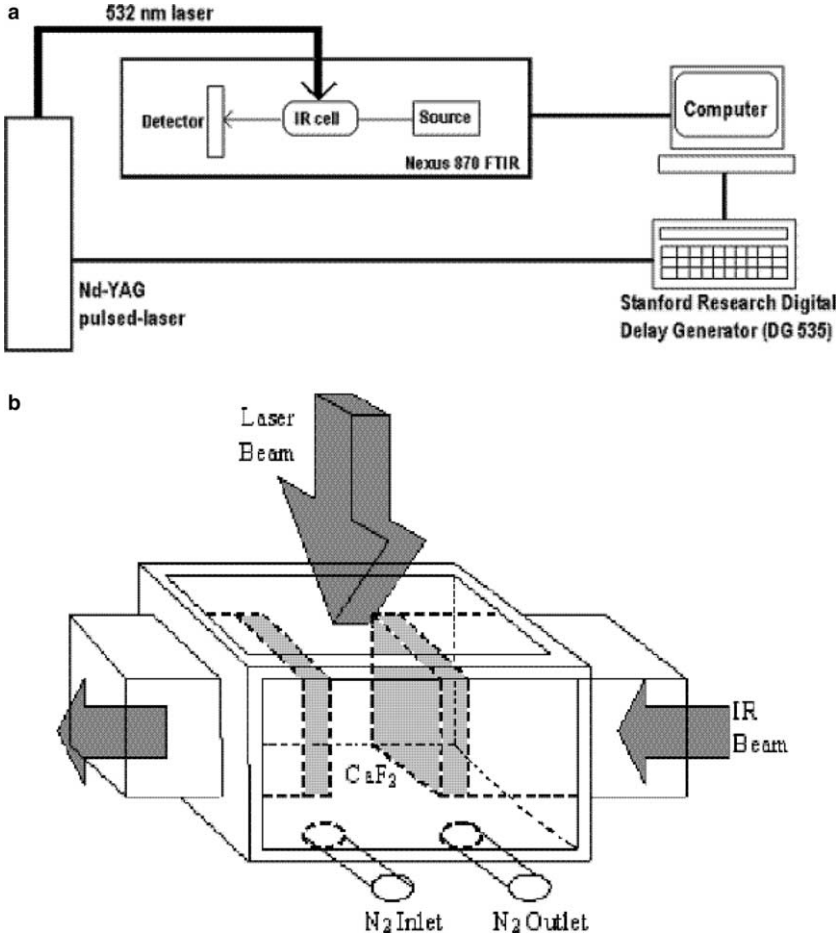

Fig. 1. (a) Schematic setup of the TRS experiment and (b) extended schematic diagram of our home-made IR cell.

solutions with additional solid precursor remaining in the reaction cell could be prepared. This would ensure continuous observation of radical signals until all the solids have dissolved and reacted. The experiments could also be performed using different mol ratio of $[CpMo(CO)_3]_2$ to halide precursors. Usually, a ratio of 1:1 was used for spectroscopic measurements although comparable radical signals have also been produced using ratios from 1:3 to 3:1. On the other hand, free phosphines (PPh_3, $P(OEt)_3$, $P(C_6F_5)_3$) were added into a solution containing $[CpMo(CO)_3]_2$ for carrying out experiments according to method 3. About 10–25 mg of the metal precursors and phosphines in 30 ml of hexane solvent were used for method 3, similar to method 2.

A frequency-doubled Q-switched Nd-YAG pulsed-laser (Continuum Surelite III-10, 532 nm, 10 Hz, 25–30 mJ/pulse, 10 ns) was focused elliptically by a cylindrical lens into the region between the CaF_2 windows in the cell for maximum overlap with the IR beam. The generation of radical signals could be optimized at higher laser energies (>30 mJ/pulse) although at such energies, the quartz windows through which the laser passed, would be damaged more quickly. For the collection of TR-FTIR spectra, an AC-coupled detector (TRS-20 MHz MCT detector) was used to capture changes in the IR absorption down to 1 μs while the synchronization of the spectrometer with the firing of the pulsed laser was controlled by a Digital Delay Generator (Stanford SRS DG 535). Radical signals could be detected most easily at short time intervals below 1 μs, i.e., before their decay fully set in after the nanosecond laser pulse has stopped firing. Although the spectrometer has the capability of recording spectra at 20 ns time interval, it was not a necessity to set the time interval to below 1 μs for spectroscopic measurements since most radicals observed here have lifetimes of a few microseconds. However for more precise kinetic studies, this feature would be essential. The detection range and resolution of a step-scan Nicolet Nexus 870 FTIR spectrometer were set at 1000–4000 and 4 cm^{-1} respectively. We have found that only one scan of the spectrum which lasted about 30 min was sufficient to produce detectable signals of the radicals [14]. We have found that averaging radical signals over a few scans only improved them slightly but at the expense of time. Linear scan FTIR measurements over the same wavelength and resolution were also carried out to record the evolution of stable species in the solution throughout the photolysis.

3. Results and discussion

3.1. Photodissociation of metal–metal bonded dimers

The ν_{CO} infrared bands of the detected radicals are presented in Table 1. Initially, the TR-FTIR spectroscopy of the previously detected $CpMo(CO)_3$ radical was carried out so that the sensitivity of the experimental setup could be tested while its chemical lifetime could also be employed as references for comparison with new radical species [10]. Unless stated otherwise, the lifetime regardless of the kinetic order of the decay, is simply defined as the time taken for the absorption intensity of the radical to decrease to half of the initial value. Having successfully identified the vibrational bands of $CpMo(CO)_3$ (1914, 2010 cm^{-1}), the TR-FTIR spectra of other radicals were then recorded. The second-order decay lifetime of $CpMo(CO)_3$ radical of 4.6 μs is also in very good agreement with previous studies in which radical–radical recombination was postulated to be its main loss process in *n*-heptane [10].

Fig. 2(a) shows an example of a TR-FTIR spectrum recorded about 10 μs after 532 nm laser photolysis of the mono-phosphine complex, $Cp_2Mo_2(CO)_5PPh_3$. Apart from the bands belonging to $CpMo(CO)_3$, two other bands at 1834 and 1924 cm^{-1} have been detected. These bands have been assigned to $CpMo(CO)_2PPh_3$ based on several observations. Metal–metal bond photolysis of $Cp_2Mo_2(CO)_5PPh_3$ should result in the simultaneous generation of these two radicals. The vibrational band positions are consistent with a shift to lower wavenumbers upon phosphine substitution of $CpMo(CO)_3$. The measured lifetime of the phosphine-containing radical (5.6 μs) was close to that of $CpMo(CO)_3$, indicating similarity in reactivity. The ν_{CO} frequencies for structurally similar stable species such as $CpMo(CO)_2PPh_3C_2H_5$ (1843, 1930 cm^{-1}) showed very good agreement with those belonging to the radical [23–26]. In fact, these analyses have been applied successfully to the identification of all the TR-FTIR radicals in Table 1 regardless of the method of generation.

A linear FTIR scan has been recorded of the reaction mixture in order to observe the formation of long-lived

Table 1
TR-FTIR spectral data of transition metal carbonyl radicals detected using one of the three methods

Method	Radicals	IR bands (cm^{-1})
1–3	$CpMo(CO)_3$	2010, 1912
1, 3	$CpMo(CO)_2PPh_3$	1924, 1834
1, 3	$CpMo(CO)_2P(OEt)_3$	1936, 1853
1, 3	$CpMo(CO)_2PMe_3$	1921, 1838
1, 2	$CpFe(CO)_2$	2004, 1938
1	$CpW(CO)_3$	2000, 1900
1	$CpW(CO)_2PPh_3$	1915, 1827
1	$Cp^*Mo(CO)_3$	1990, 1898
1	$Cp^*Mo(CO)_2PPh_3$	1961, 1840
1	$Cp^*W(CO)_3$	1984, 1887
2	$Re(CO)_5$	1996, 1977
2	$Mn(CO)_5$	1986, 1970
2	$Mn(CO)_4PPh_3$	1975, 1914
2	$Mn(CO)_4AsPh_3$	1977, 1924
2	$Mn(CO)_4SbPh_3$	1971, 1913

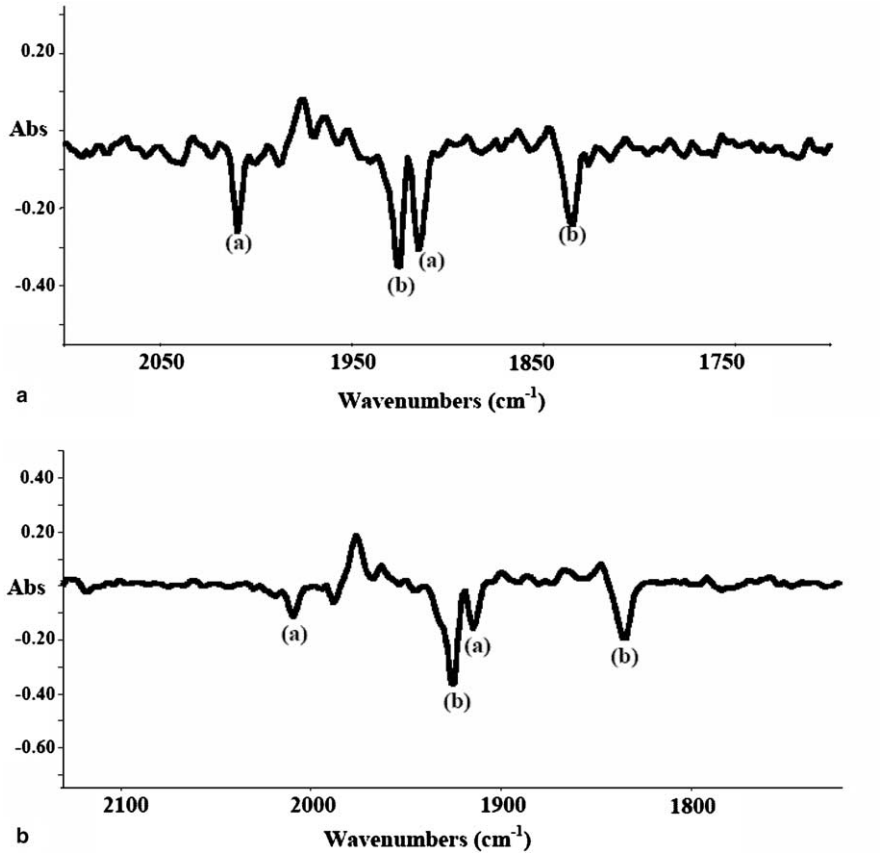

Fig. 2. TR-FTIR spectra of $CpMo(CO)_3$ (2010, 1914 cm^{-1}) and $CpMo(CO)_2PPh_3$ (1924, 1834 cm^{-1}) upon (a) $Cp_2Mo_2(CO)_5PPh_3$ metal–metal bond photolysis or (b) PPh_3 ligand substitution in the presence of $[CpMo(CO)_3]_2$. The band pointing up at 1962 cm^{-1} is due to $[CpMo(CO)_3]_2$.

metal carbonyl species during photolysis. For example, with $Cp_2Mo_2(CO)_5PR_3$ as the precursor, the linear scan revealed increased concentrations of $[CpMo(CO)_3]_2$ and $[CpMo(CO)_2\,PR_3]_2$ with concomitant decrease of precursor concentration. The formation of these dimers was due to radical–radical self-recombination processes of $CpMo(CO)_3$ and $CpMo(CO)_2PPh_3$. However it also implied that contributions to the $CpMo(CO)_3$ and $CpMo(CO)_2PR_3$ radical signals came from both precursor and the dimer products especially during the later stages of photolysis. However, when a symmetrical precursor such as $[CpMo(CO)_2(PR_3)]_2$ was used, the IR spectra appeared unchanged even after long hours of photolysis, indicating once again the dominance of radical–radical recombination pathway to regenerate the precursor. The same trend could be applied to the phosphine-derivatives of $CpW(CO)_3$ and to the Cp*-containing radicals.

Preliminary studies have shown that slightly longer lifetimes of the phosphine containing radicals (5 to 7 μs) were determined compared to that of $CpMo(CO)_3$. Steric and electronic effects due to the coordinated PR_3 on the recombination rate of these radicals appear not to be very significant. These results suggest that the orientation of the phosphine groups in the radicals relative to the radical recombination trajectory is most likely similar to the alkylated counterparts or the metal dimers themselves, i.e., these PR_3 groups do not restrict or block the approach of another radical species for recombination. Similar observations could also be ascribed to the Cp*-containing radicals. Since a small activation barrier for the recombination process is implied by these measurements, diffusion-limited kinetics could also have played a major role in determining the lifetimes of the radicals.

3.2. Halogen abstraction by $CpMo(CO)_3$ radicals

In this method the $CpMo(CO)_3$ radical generated upon 532 nm photolysis of $[CpMo(CO)_3]_2$ has been used to abstract the halogen atom from the transition metal carbonyl halide precursors to form ML_n radicals.

$$CpMo(CO)_3 + ML_nX \rightarrow ML_n + CpMo(CO)_3X$$
$$(X = \text{halogen},\ L = \text{other ligands})$$

The infrared ν_{CO} bands and the lifetimes of the organometallic radicals detected via halogen abstraction are also shown in Table 1. For example, the TR-FTIR spectrum recorded about 1 μs after 532 nm laser photolysis of a mixture containing $Mn(CO)_5Br$ and $[CpMo(CO)_3]_2$ showed vibrational bands due to $Mn(CO)_5$, $CpMo(CO)_3$

and *gauche*-[CpMo(CO)$_3$]$_2$ (Fig. 3). Bands belonging to the CpMo(CO)$_3$ dimer and the mixed-metal complex CpMo(CO)$_3$–Mn(CO)$_5$ were also observed but pointed to the opposite direction of the spectrum which indicated their formation upon radical–radical recombination processes.

The identity of the newly formed radicals could be made by examining their chemical lifetimes, effect of ligand substitution on the vibrational frequencies and comparisons to structurally similar 18-electron alkyl counterparts [27–32]. In the CpMo(CO)$_3$/Mn(CO)$_5$Br system for example, a band at 1986 cm^{-1} has been observed close to the literature values for Mn(CO)$_5$ ($\nu = 1988$ cm^{-1}, cyclohexane; 1990 cm^{-1}, heptane) [27,28]. The band did not show up if either Mn(CO)$_5$Br or CpMo(CO)$_3$ dimer was removed. Its short lifetime of about 8.1 μs also suggested a radical species as the carrier and thus this band was assigned to Mn(CO)$_5$. In addition, a weaker second band at 1970 cm^{-1} could also be assigned to Mn(CO)$_5$ based on the same kinetic behavior.

The halogen abstraction method of producing Mn(CO)$_5$ radical can be compared to the case where metal–metal bond photodissociation of Mn$_2$(CO)$_{10}$ was used instead. Because of the absence of strong electronic transitions in the visible region (>420 nm), the dimer is normally photolysed at uv wavelengths where the competitive decarbonylation pathway produces significant amount of Mn$_2$(CO)$_9$ [27–30]. In our case, a search for Mn$_2$(CO)$_9$ based on the previously obtained IR values turned out to be unsuccessful since halogen abstraction by CpMo(CO)$_3$ is not expected to promote decarbonylation.

A close examination of the decay curve of CpMo(CO)$_3$ and Mn(CO)$_5$ in Fig. 4(a) shows that they fit better to a first-order rather than a second-order decay. In the absence of other species, the main loss process for Mn(CO)$_5$ is its self-recombination to form Mn$_2$(CO)$_{10}$. The presence of CpMo(CO)$_3$ species obviously renders the kinetic data to be more difficult to interpret since it could also combine efficiently with Mn(CO)$_5$. Indeed the mixed metal complex, CpMo(CO)$_3$–Mn(CO)$_5$ observed in the system most likely came from the cross-radical recombination reaction.

We have found that reactions between CpMo(CO)$_3$ and many transition metal carbonyl halides were not reversible although this condition is essential for acquiring TR-FTIR spectra in a static cell. Choosing the CpMo(CO)$_3$/Mn(CO)$_5$Br (1:1 mole ratio) system as an example, the linear scan FTIR spectroscopy recorded of the reaction mixture two hours after photoinitiation only indicated the presence of Mn$_2$(CO)$_{10}$, CpMo(CO)$_3$Br and a lesser amount of the mixed-metal complex, CpMo(CO)$_3$–Mn(CO)$_5$; all of which are not susceptible to 532 nm photolysis (see Fig. 4(b)) [33–35]. For such cases, TR-FTIR signals of Mn(CO)$_5$ and CpMo(CO)$_3$ species should also gradually decrease as the photolysis progresses towards completion. Indeed TR-FTIR spectra taken at later stages of photolysis showed much lower signals of both radicals, consistent with the linear scan measurements.

Similar results were obtained for the CpMo(CO)$_3$/CpFe(CO)$_2$I system. Although 532 nm photodissociation of the [CpFe(CO)$_2$]$_2$ product is possible, reversibility could not be achieved because of inefficient iodine atom abstraction by CpFe(CO)$_2$ from the CpMo(CO)$_3$I product. We conclude that at least for the Mn/Mo and Mo/Fe systems, the reverse abstraction process is

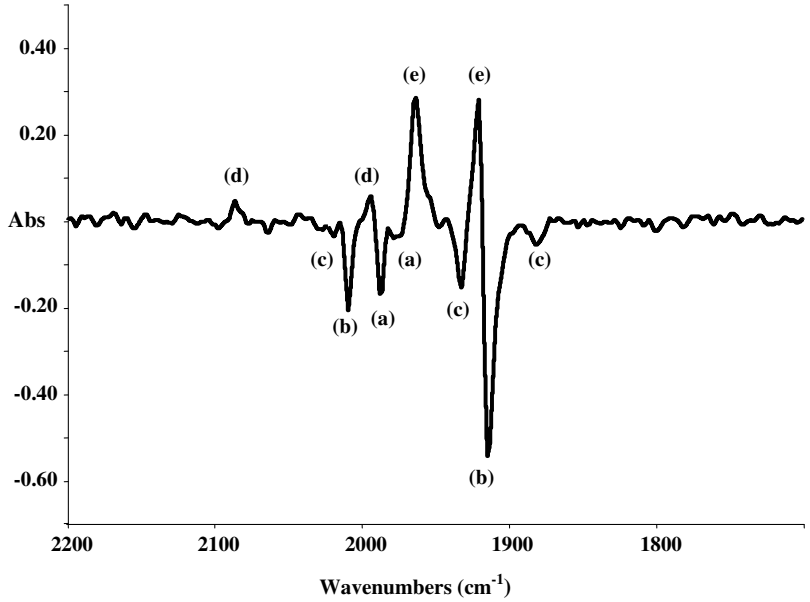

Fig. 3. TRS data (1 μs after laser pulse) shows the production of (a) Mn(CO)$_5$ at 1988 and 1973 cm^{-1}, (b) CpMo(CO)$_3$ at 2010 and 1914 cm^{-1}, (c) *gauche*-[CpMo(CO)$_3$]$_2$ at 2020, 1932 and 1880 cm^{-1}, (d) CpMo(CO)$_3$–Mn(CO)$_5$ at 2085 and 1994 cm^{-1} from 532 nm photolysis of (e) *trans*-[CpMo(CO)$_3$]$_2$ and excess of Mn(CO)$_5$Br in hexane solution via halide abstraction.

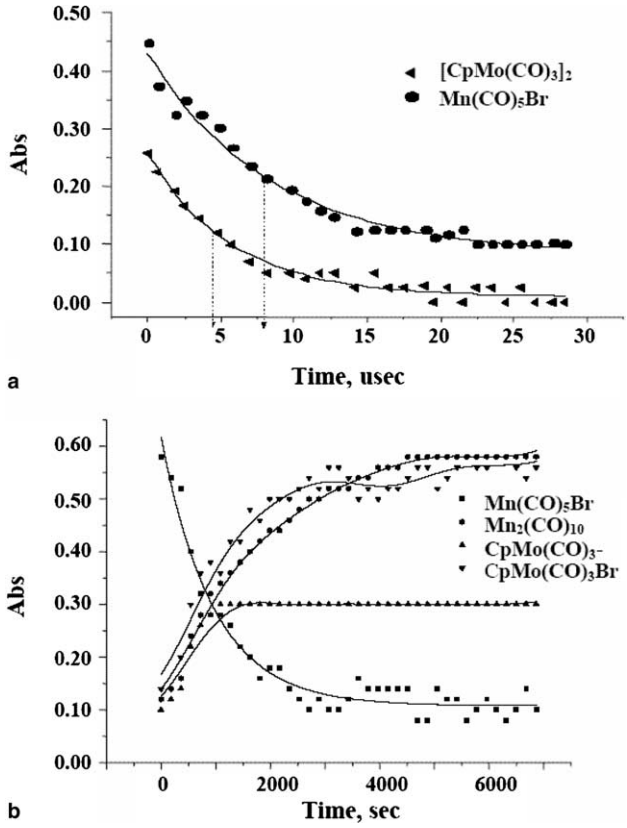

Fig. 4. (a) The TR-FTIR decay curves of $CpMo(CO)_3$ (◀) and $Mn(CO)_5$ (●) radicals and (b) the spectral changes of stable organometallic components during the halide abstraction process in the $[CpMo(CO)_3]_2/Mn(CO)_5Br$ system.

endothermic enough to prevent any overall reaction reversibility. Nevertheless, we have shown here that the reversibility conditions need not be maintained or even required in order to detect TR-FTIR radical signals. Optimal signals are best acquired during the initial stages of photolysis while the reactants are still present in large amount.

3.3. Radical ligand substitution

Detection of TR-FTIR spectra of transition metal carbonyl radicals via fast ligand substitution is also possible. Fig. 2(b) shows the TR-FTIR spectrum of $CpMo(CO)_2PPh_3$ generated together with $CpMo(CO)_3$ upon $[CpMo(CO)_3]_2$ photolysis in the presence of excess PPh_3 (>3:1) in hexane. As expected the same radical species were expected to be detected via this method when compared to those obtained by method 1, i.e., metal–metal bond dissociation of $Cp_2Mo_2(CO)_5PPh_3$ (Fig. 2(a)). A linear FTIR scan showed fast depletion of $CpMo(CO)_3$ dimer signals upon photolysis accompanied by facile formation of its mono and diphosphine derivatives. Initially we thought that the substitution proceeded via the decarbonylation product, $Cp_2\ Mo_2(CO)_5$ but no evidence of it was seen even when pure $[CpMo(CO)_3]_2$ was photolysed at 532 nm. However disproportionation reactions induced by uv photolysis of the dimer have been shown to lead to ionic phosphine-containing complexes in polar solvents [36]. The formation of the PPh_3- containing products in hexane is more likely due to fast phosphine ligand substitution into $CpMo(CO)_3$ itself. Trogler [37] has reviewed similar substitution processes for $V(CO)_6$ and $Mn(CO)_5$ radicals in which facile formation of a two-center three-electron bond where the odd electron interacts with an electron pair on an entering nucleophile, can lead to large substitution rates. In our case, it appears that $CpMo(CO)_3$ radical kinetics conform to this trend although further phosphine substitution into the $CpMo(CO)_2PPh_3$ radical is either very slow or does not take place.

The decay lifetimes measured for both $CpMo(CO)_3$ (4.8 μs) and $CpMo(CO)_2PPh_3$ (5.5 μs) in a 1:1 $[CpMo(CO)_3]_2/PPh_3$ system are essentially the same as those obtained via method 1. This is probably not surprising because the radicals were produced under rather similar chemical environment especially during the later stages of photolysis. Since the latter radical must have originated from $CpMo(CO)_3$, there should be a difference in the appearance or risetime of both radicals. We have been unable to observe the differences presumably because the ligand substitution reaction proceeded too quickly. However the subsequent generation of $CpMo(CO)_2PPh_3$ during the later stages of the TR-FTIR scan came from photodissociation of the mono and diphosphine-substituted molybdenum complex. The linear FTIR kinetic scan shows that it takes only a short while (<10 min, 25 mJ laser energy) for a significant amount of the dimeric phosphine derivatives to build up at the expense of the $CpMo(CO)_3$ dimer. However, depending on the relative donor strength, not all phosphines can be substituted into the $CpMo(CO)_3$ radical. For example, both $CpMo(CO)_3$ and $CpMO(CO)_2(POEt_3)$ radical signals could be observed while the presence of only $CpMo(CO)_3$ signals were detected when $P(C_6F_5)_3$ was used instead.

3.4. Comparison

The three methods used for TR-FTIR radical detection are briefly assessed. Photodissociation of metal-bonded dimers (method 1) is straightforward with interpretable radical–radical recombination kinetics. It is the only method described here where reversible kinetics could be achieved. However, unless the metal-bonded dimers are commercially available, syntheses of the dimers have to be carried out but interpretation of the kinetics data could be brought into question if there are significant synthetic side products. Low quantum yields and decarbonylation pathways upon metal–metal bond dissociation are also among some factors causing low radical concentrations.

Halogen abstraction by $CpMo(CO)_3$ radical is the most versatile of the three methods presented here. Many transition metal carbonyl halides are commercially available, relatively air stable and easily derivatized with phosphines and other two-electron donors. The long wavelength required to produce $CpMo(CO)_3$ also prevents extensive halide photodecomposition. While the abstraction process works well for first row halides, it could be difficult to apply to later row species such as $CpRu(CO)_2Cl$ and (Indenyl)$Ru(CO)_2I$. We have failed to carry out halogen abstraction of these ruthenium species by $CpMo(CO)_3$ presumably due to the stronger ruthenium–halide bond. Compared to the first method, the interpretation of the irreversible halogen abstraction process could be more difficult as well.

Radical ligand substitution (method 3) is excellent for generating spectroscopic data of phosphine-containing transition metal carbonyl radicals. Unlike method 1, the syntheses of high purity phosphine-containing metal-bonded precursors are not required. Ligand substitution rate studies have so far been restricted to a very few classes of radicals. We hope to provide some impetus for such studies since both radicals before and after substitution could be directly detected and characterized. Obviously the shortcomings are reflected in a more complicated kinetic scheme in which nanosecond TR-FTIR timescale may not be sufficiently short to detect differences in the risetime between the two radicals. A picosecond TR-FTIR system will be of more general use for such measurements.

The three methods used here have widened the scope for spectroscopic detection of transition metal carbonyl radicals. All three methods should be exploited in a complementary manner so that a thorough understanding of the spectroscopy and kinetics of transition metal carbonyl radicals could be achieved. The requirement of complete reversibility in the reactions is also not necessary if methods 2 and 3 were employed, hence reducing considerable amount of time in devising such reaction schemes for TR-FTIR studies. Work is already underway to understand in detail the kinetics of the reactions carried out according to all three methods. We also plan to record spectra of radical species directly implicated in homogeneous catalytic process as well as radicals that contain two-electron donors such as isocyanides and Arduengo carbenes.

Acknowledgements

This work was supported by the Agency of Science, Technology and Research (ASTAR) under Metallocene Catalysis Grant No. 012-101-0035. T.S. Chong thanked the Institute of Chemical and Engineering Science (ICES) of Singapore for a research scholarship.

References

[1] M.S. Wrighton, Chem. Rev. 74 (1974) 401.
[2] M.C. Baird, Chem. Rev. 88 (1988) 1217.
[3] M. Poliakoff, E. Weitz, Adv. Organomet. Chem. 25 (1986) 277.
[4] M.W. George, M. Poliakoff, J. Turner, J. Anal. 119 (1994) 551.
[5] H. Hermann, F.W. Grevels, A. Henne, K. Schaffner, J. Phys. Chem. 86 (1982) 5151.
[6] Y. Ishikawa, P.A. Hackett, D.M. Rayner, J. Mol. Struct. 174 (1988) 113.
[7] A.J. Dixon, M.A. Healy, P.M. Hodges, B.D. Moore, M. Poliakoff, M.B. Simpson, J.J. Turner, M.A. West, J. Chem. Soc., Faraday Trans. 2 82 (1986) 2083.
[8] A.J. Dixon, M.W. George, C. Hughes, M. Poliakoff, J.J. Turner, J. Am. Chem. Soc. 114 (1992) 1719.
[9] B.D. Moore, M.B. Simpson, M. Poliakoff, J.J. Turner, J. Chem. Soc. Chem. Commun. 15 (1984) 972.
[10] J. Peters, M.W. George, J. Turner, J. Organomet. 14 (1995) 1503.
[11] I.G. Virrels, M.W. George, F.P.A. Johnson, J.J. Turner, J.R. Westwell, Organometall. 14 (1995) 5203.
[12] X.Z. Sun, S.M. Nikiforov, A. Dedieu, M.W. George, Organometall. 20 (2001) 1515.
[13] B.D. Moore, M. Poliakoff, M.B. Simpson, J.J. Turner, J. Phys. Chem. 89 (1985) 850.
[14] X.Z. Sun, S.M. Nikiforov, J. Yang, C.S. Colley, M.W. George, Appl. Spectrosc. 56 (2002) 31.
[15] M. Jezequel, V. Dufaud, M.J. Ruiz-Garcia, F. Carrillo-Hermosilla, U. Neugebauer, G.P. Niccolai, F. Lefebvre, F. Bayard, J. Corker, S. Fiddy, J. Evans, J.P. Broyer, J. Malinge, J.M. Basset, J. Am. Chem. Soc. 123 (2001) 3520.
[16] S.L. Buchwald, E.V. Anslyn, R.H. Grubbs, J. Am. Chem. Soc 107 (1985) 1766.
[17] S.J. Sturla, N.M. Kablaoui, S.L. Buchwald, J. Am. Chem. Soc. 121 (1999) 1976.
[18] R.J. Haines, C.R. Nolte, J. Organomet. Chem. 24 (1970) 725.
[19] D.S. Ginley, C.R. Bock, M.S. Wrighton, Inorg. Chim. Acta 23 (1977) 85.
[20] J. Wachter, J.G. Riess, A. Mitschler, Organometallics 3 (1984) 714.
[21] W. Hieber, G. Faulhaber, F. Theubert, Z. Anorg. Allg. Chem. 314 (1962) 125.
[22] R.J. Angelici, F. Basolo, J. Am. Chem. Soc. 84 (1962) 2495.
[23] H.G. Alt, M.E. Eichner, J. Organomet. Chem. 212 (1981) 397.
[24] R.H. Hill, J.D. Debad, Polyhedron 10 (1991) 1705.
[25] O.G. Adeyemi, N. Coville, J. Organomet. 22 (2003) 2284.
[26] A.S. Goldman, D.R. Tyler, J. Am. Chem. Soc. 108 (1986) 89.
[27] S.P. Church, H. Hermann, F.W. Grevels, K. Schaffner, J. Chem. Soc. Chem. Commun. 12 (1984) 785.
[28] S.P. Church, M. Poliakoff, J.A. Timney, J.J. Turner, J. Am. Chem. Soc. 103 (1981) 7515.
[29] S. Firth, P.M. Hodges, M. Poliakoff, J. Turner, J. Inorg. Chem. 25 (1986) 4608.
[30] H. Yesaka, T. Kobayashi, K. Yasufuku, S. Nagakura, J. Am. Chem. Soc. 105 (1983) 6249.
[31] C.S. Kraihanzel, P.K. Maples, J. Am. Chem. Soc. 87 (1965) 5267.
[32] C.S. Kraihanzel, P.K. Maples, Inorg. Chem. 7 (1968) 1806.
[33] T. Madach, H. Vahrenkamp, Chem. Ber. 113 (1980) 2675.
[34] R.H. Hill, A. Becalska, N. Chiem, Organometallics 10 (1991) 2104.
[35] W. Xia, L.B. Goetting, J.D. Debad, B.J. Palmer, R.H. Hill, J. Photochem. Photobiol. A 71 (1993) 221.
[36] C.E. Philbin, A.S. Goldman, D.R. Tyler, Inorg.Chem. 25 (1986) 4434.
[37] W.C. Trogler, Int. J. Chem. Kinet. 19 (1987) 1025.